

# Pitfalls and prospects of optical spectroscopy to characterize perovskite-transport layer interfaces <sup>EP</sup>

Cite as: Appl. Phys. Lett. **116**, 100501 (2020); <https://doi.org/10.1063/1.5143121>

Submitted: 20 December 2019 . Accepted: 18 February 2020 . Published Online: 09 March 2020

Eline M. Hutter <sup>id</sup>, Thomas Kirchartz <sup>id</sup>, Bruno Ehrler <sup>id</sup>, David Cahen <sup>id</sup>, and Elizabeth von Hauff <sup>id</sup>

## COLLECTIONS

<sup>EP</sup> This paper was selected as an Editor's Pick



View Online



Export Citation



CrossMark

Lock-in Amplifiers  
Find out more today



 Zurich Instruments

# Pitfalls and prospects of optical spectroscopy to characterize perovskite-transport layer interfaces EP

Cite as: Appl. Phys. Lett. **116**, 100501 (2020); doi: [10.1063/1.5143121](https://doi.org/10.1063/1.5143121)

Submitted: 20 December 2019 · Accepted: 18 February 2020 ·

Published Online: 9 March 2020



View Online



Export Citation



CrossMark

Eline M. Hutter,<sup>1,a)</sup> Thomas Kirchartz,<sup>2,3</sup> Bruno Ehrler,<sup>1</sup> David Cahen,<sup>4,5</sup> and Elizabeth von Hauff<sup>1,6,b)</sup>

## AFFILIATIONS

<sup>1</sup>Center for Nanophotonics, AMOLF, Science Park 104, 1098 XG Amsterdam, The Netherlands

<sup>2</sup>IEK-5 Photovoltaik, Forschungszentrum Jülich, 52425 Jülich, Germany

<sup>3</sup>Faculty of Engineering and CENIDE, University of Duisburg-Essen, Carl-Benz-Str. 199, 47057 Duisburg, Germany

<sup>4</sup>Department of Materials and Interfaces, Weizmann Institute of Science, Rehovoth 76100, Israel

<sup>5</sup>Department of Chemistry and Bar-Ilan Institute of Nanotechnology and Advanced Material, Bar-Ilan University, 5290002 Ramat Gan, Israel

<sup>6</sup>Department of Physics and Astronomy, VU Amsterdam, De Boelelaan 1081, 1081 HV Amsterdam, the Netherlands

<sup>a)</sup>Present address: Debye Institute for Nanomaterials Science, Princetonlaan 8, 3584 CB, Utrecht, The Netherlands.

<sup>b)</sup>Author to whom correspondence should be addressed: [e.l.von.hauff@vu.nl](mailto:e.l.von.hauff@vu.nl)

## ABSTRACT

Perovskite photovoltaics has witnessed an unprecedented increase in power conversion efficiency over the last decade. The choice of transport layers, through which photo-generated electrons and holes are transported to electrodes, is a crucial factor for further improving both the device performance and stability. In this perspective, we critically examine the application of optical spectroscopy to characterize the quality of the transport layer-perovskite interface. We highlight the power of complementary studies that use both continuous wave and time-resolved photoluminescence to understand non-radiative losses and additional transient spectroscopies for characterizing the potential for loss-less carrier extraction at the solar cell interfaces. Based on this discussion, we make recommendations on how to extrapolate results from optical measurements to assess the quality of a transport layer and its impact on solar cell efficiency.

Published under license by AIP Publishing. <https://doi.org/10.1063/1.5143121>

Over the last decade, metal-halide perovskite photovoltaics (PV) has demonstrated an unprecedented increase in power conversion efficiencies, from  $\sim 4\%$ <sup>1</sup> in 2009 to  $\sim 25\%$  in 2019.<sup>2</sup> The impressive increase in efficiency over time is partially due to the unique material properties of perovskite absorber layers, such as the low density of defect states in the bandgap.<sup>3</sup> This low defect density is particularly remarkable given that the films used for photovoltaics are polycrystalline layers processed from solution near room temperature. The low defect density yields sharp absorption onsets and relatively high emission quantum yields (QY).<sup>4,5</sup> Furthermore, tuning of the optical bandgap via varying the precursor composition allows for solar cell architectures that harvest more of the energy in the solar spectrum, such as tandem solar cells. On the other hand, progress must also be attributed to the enormous global efforts by researchers with a variety of expertise, toward the fabrication, characterization, and engineering of high-performance energy-conversion and light-emitting devices.

The commercial feasibility of a PV technology can be qualitatively assessed based on the interplay between efficiency, cost, and lifetime. Perovskite solar cells score high on the first two points so that improving material and device stability remains one of the largest challenges for the field. The choice of *transport layers*, through which photo-generated electrons and holes are transported to the electrodes, is a crucial factor for device performance<sup>6,7</sup> and stability.<sup>8</sup> Analogous to the development history of other PV technologies, this critical step in device engineering has motivated the perovskite PV community to search for ideal transport layer materials that are Ohmic for one carrier type to prevent performance losses during charge extraction. The concept of *selective contacts* is well-known in PV,<sup>8–11</sup> in particular for the doped silicon transport layers in high performance silicon PV.<sup>12</sup> In contrast, the development of selective contacts in thin film PV has been more challenging.<sup>13</sup> This is because the requirements for a transport layer to be considered *selective* are strict; selective transport layers should allow extraction of only one charge carrier without causing

additional resistive loss (i.e., should form an Ohmic contact for current of one charge carrier type) and prevent electrical losses caused, e.g., by a decrease in carrier mobility at the contact<sup>14</sup> or interfacial non-radiative recombination due to trapping and minority carrier recombination. In addition to the requirement of selectivity, transport layers also have to be designed to minimize optical losses such as parasitic absorption.<sup>15</sup> All of these losses will ultimately reduce the power conversion efficiency of the solar cell. Sometimes, the term “extraction layer” is used in connection with transport materials that facilitate charge collection from the active layer. However, it is important to note that selective transport layers are *passive*, i.e., they simply form a loss-less contact between the semiconductor absorber layer and the metal contact for one of the charges (electron or hole), while the other charge is blocked by a sufficiently large barrier ( $\Delta E \gg kT$ ). In other words, an ideal selective contact performs the simple, yet elusive, task of prohibiting electrical (non-radiative recombination) losses during carrier extraction.

In the case of thin-film PV such as perovskite PV, where the interfaces between the absorber and transport layers are formed by two different materials (heterojunction), a physico-chemical understanding of the interfacial properties is a prerequisite toward the rational design of efficient and stable solar cells. Therefore, engineering optimized architectures requires understanding of the energy level alignment and electric field distribution within the solar cell and of the recombination channels in the absorber layer and at the device interfaces.

In this perspective, we specifically address the question of how to screen and characterize the quality of the interfaces between transport layers and perovskite absorbers. *In situ* characterization tools are especially suitable for studying the optoelectronic properties of solar cell interfaces under conditions that are relevant for real applications, such as variations in the absorber composition, different environmental stress factors, and aging during device operation. We highlight the advantages and challenges in using photoluminescence (PL) spectroscopy, also in conjunction with other optical spectroscopies, to specifically target device interfaces for the screening of new transport layers. Selective transport layers should ideally not induce additional loss channels and hence not affect the photoluminescence quantum yield ( $Q_e^{\text{PL}}$ ) nor lead to a reduction in the energy of the excited state. A red-shift in the energy of the PL spectrum is associated with a loss in carrier energy and in turn a loss in the open circuit voltage ( $V_{\text{oc}}$ ) of the solar cell. Therefore, the  $Q_e^{\text{PL}}$  and spectral shape of the emission from the perovskite active layer should ideally remain unchanged when interfaced with the transport layer. This means that, in principle, a steady-state, or continuous wave (cw), PL measurement may be sufficient to screen the passivation quality of new transport layers. However, using both steady-state and time-resolved (tr) spectroscopy and combining these with electrical measurements are more suitable to study the contacts' selectivity and to derive quantitative information about the opto-electronic processes in the sample, including carrier densities, lifetimes, and charge-transfer rates at material interfaces. Such an approach is needed not only for understanding but also for guiding material and device fabrication protocols.

Here, we highlight the power of complementary studies that use both cw-PL and tr-PL to understand non-radiative losses and additional transient spectroscopies for characterizing the potential for loss-less carrier extraction at the solar cell interfaces.<sup>16</sup> Based on our

discussion, we make recommendations on how to extrapolate results from optical measurements to assess the quality of a transport layer and its impact on solar cell efficiency.

We now discuss how to assess the interfacial quality between the perovskite and transport layer by applying PL quenching as a signature of non-radiative losses. The model originally proposed by Shockley and Queisser,<sup>17</sup> i.e., the SQ model, defines an ideal solar cell as a cell that fulfills several idealized assumptions,<sup>18</sup> which include most notably the absence of any non-radiative recombination processes. Hence, an ideal solar cell has a steady-state photoluminescence emission quantum efficiency ( $Q_e^{\text{PL}}$ ) of unity. The SQ model additionally assumes that each absorbed photon produces one electron-hole pair that rapidly thermalizes to the band edges. At  $V_{\text{oc}}$ , no net photocurrent flows, and the absorption of radiation is balanced by the emission of radiation at the bandgap energy; thus, in this limit, all photo-generated charge recombines radiatively. In order to maximize the efficiency of a solar cell toward the SQ limit, one should aim for this ideal scenario in which there are neither losses due to non-radiative recombination nor losses in energy due to unfavorable band alignments. This is also known as the *radiative limit*. Figure 1 shows ideal ( $k_R$ ) and non-ideal ( $k_{\text{NR}}$ ) recombination processes. For an extensive description of the physics of solar cells, we refer to, for example, Nelson<sup>19</sup> and Würfel.<sup>20</sup>

In real semiconductors, the chemical potential of the photo-generated electrons and holes in this quasi-equilibrium scenario can be represented by the splitting of the quasi-Fermi levels of the electrons and holes. This quasi-Fermi level splitting (QFLS) is directly related to the density of photo-generated electrons and holes<sup>21,22</sup> and sets an upper limit for the  $V_{\text{oc}}$  of the solar cell.

If the quasi-Fermi levels are flat across the absorber layer, then the luminescence efficiency depends on applied voltage but not on the source of excitation. Thus, the external photoluminescence and electroluminescence quantum efficiencies will be the same ( $Q_e^{\text{PL}} = Q_e^{\text{EL}}$ ).

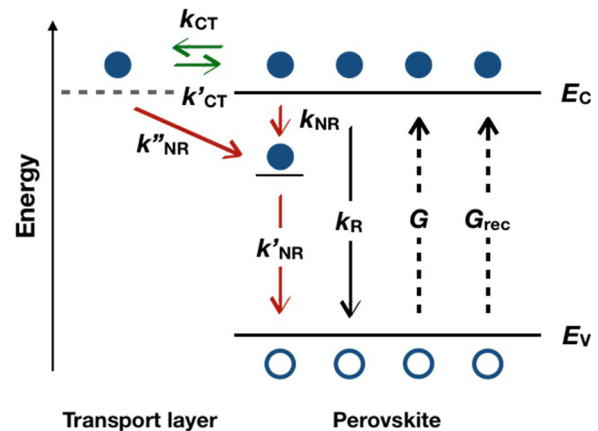


**FIG. 1.** Optical excitation of the absorber leads to generation (G) of photocarriers. Carriers ideally recombine radiatively ( $k_R$ ) via band-to-band recombination. Photon recycling results in further generation of carriers ( $G_{\text{rec}}$ ). At the interface between the perovskite and transport layer, charge transfer ( $k_{\text{CT}}$ ) processes that are associated with the corresponding back transfer of charge ( $k'_{\text{CT}}$ ) do not reduce the cw-PL intensity but will affect  $\Delta n(t)$  and may thus be observed in the tr-PL spectrum. Non-radiative losses, such as defect-assisted recombination due to traps in the bulk active layer ( $k_{\text{NR}}$ ,  $k'_{\text{NR}}$ ) or at the interface between the active layer and the transport layer ( $k''_{\text{NR}}$ ) will reduce the PLQY.

In this scenario, any loss in the solar cell  $V_{oc}$  is quantitatively correlated with losses in the external luminescence quantum efficiency  $Q_e^{PL}$  via<sup>23</sup>

$$V_{oc} = V_{oc}^{rad} + \frac{kT}{q} \ln(Q_e^{PL}), \quad (1)$$

meaning that each decade of loss in  $Q_e^{PL}$  relates to a voltage loss of about 60 meV. Here,  $kT/q$  is the thermal voltage (25.8 mV at 298 K, room temperature, RT) and  $V_{oc}^{rad}$  is the open-circuit voltage in the radiative limit (i.e., if all charges undergo radiative recombination).<sup>15</sup> Furthermore, in the limit of flat quasi-Fermi levels across the absorber, we can quantify the relationship between the external luminescence quantum efficiency  $Q_e^{PL}$  and the internal luminescence quantum efficiency  $Q_i^{lum}$ . The internal luminescence quantum efficiency is the ratio of the radiative and total recombination rates ( $Q_i^{lum} = R_R/R_{tot}$ ) and is related to  $Q_e^{PL}$  via the outcoupling efficiency  $p_e$  and the probability  $p_r$  of photon reabsorption by the absorber, which can lead to photon recycling<sup>15</sup>

$$Q_e^{PL} = \frac{p_e Q_i^{lum}}{1 - p_r Q_i^{lum}}. \quad (2)$$

Thus, to achieve the ideal  $V_{oc}$  predicted by the radiative limit, every photon emitted by the absorber layer has to be either out-coupled or reabsorbed by the absorber layer itself.<sup>24,25</sup>

In addition to non-radiative recombination, substantial losses can occur from the parasitic absorption of (emitted) photons by the transport materials or metal electrodes. In real solar cells, quenching of the cw-PL resulting in  $Q_e^{PL} < 1$  is associated with non-ideal, i.e., non-radiative losses and therefore a reduction in  $V_{oc}$ . In the literature, many studies demonstrate relatively good  $Q_e^{PL}$  values for perovskite layers deposited onto insulating substrates, such as glass. These layers are often passivated either by controlled exposure to oxygen or by covering them with passivation layers, such as poly(methyl-methacrylate) (PMMA) or n-triethylphosphine oxide (TOPO).<sup>26,27</sup> In contrast, there are few cw-PL studies showing high  $Q_e^{PL}$  from perovskites interfaced with suitable *conductive* transport layers.<sup>28,29</sup> While there is little question that high  $Q_e^{PL}$  is indicative of high material quality in perovskite thin films on glass, a decrease in the cw-PL intensity for a perovskite layer interfaced with a conductive charge-transport layer is often erroneously interpreted as a desirable phenomenon for a high efficiency solar cell.

In fact, in the case of perovskite-transport layer interfaces, PL quenching has led to some contradictory interpretations. Some reports interpret PL quenching as a signature of efficient charge transfer,<sup>30</sup> while other reports correlate reduced PL intensity with non-radiative losses, such as surface recombination.<sup>31</sup> Part of this confusion may be linked to the fact that in the field of organic photovoltaics (a field in which many perovskite PV researchers were previously active), PL quenching has long been interpreted as a sign of efficient charge separation at the molecular donor-acceptor interface. However, also in these systems, quenching of the singlet emission from the donor molecule corresponds to a loss in carrier energy because it is associated with the formation of the localized, weakly emissive charge transfer state at the donor-acceptor interface.<sup>32–34</sup> This means that in addition to loss in carrier energy upon charge transfer, there is also a loss in emission from the device. Both effects ultimately limit the solar cell  $V_{oc}$ .

Clearly, in the context of the radiative limit, *device interfaces should not quench the PL* of the absorber layer, so as to allow high open circuit voltages from devices. Furthermore, charge transfer and extraction cannot be probed under steady-state open-circuit conditions, under which the net current flow in the device is zero. Instead, charge extraction can either be probed using PL spectroscopy away from  $V_{oc}$ <sup>35–37</sup> or, as we discuss later, by using other transient techniques. This means that cw-PL performed at open-circuit conditions can only yield insight into how a given transport layer influences the  $Q_e^{PL}$  of the perovskite absorber. Insulating, passivating layers<sup>27</sup> may yield high  $Q_e^{PL}$  but will not allow charge extraction. Only the combination of both high  $Q_e^{PL}$  (which is measured at the open circuit) and low series resistance (which can only be measured away from the open circuit) is a sufficient condition for establishing that a given transport layer forms a suitable selective contact with the perovskite absorber. We note that fill factors around 80% in combination with negligible PL quenching have already been reported for a layer stack, using poly(triarylamine) (PTAA) as the hole transport material and phenyl-C61-butyric acid methyl ester (PCBM) as the electron transport material,<sup>29</sup> or with a passivating monolayer, self-assembled on oxide-based transport layers.<sup>38</sup> Thus, a very good compromise between efficient charge extraction and good surface passivation is fundamentally possible. The use of cw and tr-PL to study and distinguish between ideal and non-ideal recombination processes is described in more detail below. In general, the excitation intensities and conditions used for transient and continuous excitation methods are quite different and so are the subsequent carrier generation and recombination rates. Therefore, comparing the results and subsequently drawing conclusions about processes occurring under standard solar cell working conditions requires care.<sup>16</sup>

We now consider how  $V_{oc}$  can be predicted from time-resolved photoluminescence. While cw-PL is a fast way to screen non-radiative losses, tr-PL can yield insights into the rates of these processes.<sup>39</sup> These rates can then be used to predict the upper limit for the device  $V_{oc}$  as a function of perovskite composition or its contact with a specific charge transport layer, as detailed below.<sup>40–43</sup> First, it is important to understand that the excitation density has a significant effect on the recombination lifetime, and for this reason, transient measurements are commonly performed as a function of excitation intensity. In transient measurements, the time-dependent values of the photo-generated electron density  $\Delta n$  (hole density  $\Delta p$ ) take the general form

$$\begin{aligned} \frac{d\Delta n(t)}{dt} &= G - R_R - R_{NR} + G_{rec} \\ &= G - k_R \Delta n(t) \Delta p(t) - k_{NR} \Delta n(t) + p_r k_R \Delta n(t) \Delta p(t), \end{aligned} \quad (3)$$

where  $G$ ,  $R_R$ , and  $R_{NR}$  represent the rates of charge carrier generation, radiative recombination, and non-radiative recombination, respectively, as schematically depicted in Fig. 1. The recycling of emitted photons leads to an additional generation term  $G_{rec}$  ( $=p_r R_R$ ). Equation (3) ignores third-order recombination, typically observed at  $>10^{17} \text{ cm}^{-3}$ , and assumes an intrinsic semiconductor. This is a fair assumption for halide perovskites, in which the background doping levels are typically much smaller ( $<10^{12} \text{ cm}^{-3}$ )<sup>44</sup> than the excitation density at 1 sun ( $10^{15} \text{ cm}^{-3}$ ).<sup>42</sup> However, the model will be more complicated for highly doped semiconductors. All rates are dependent on



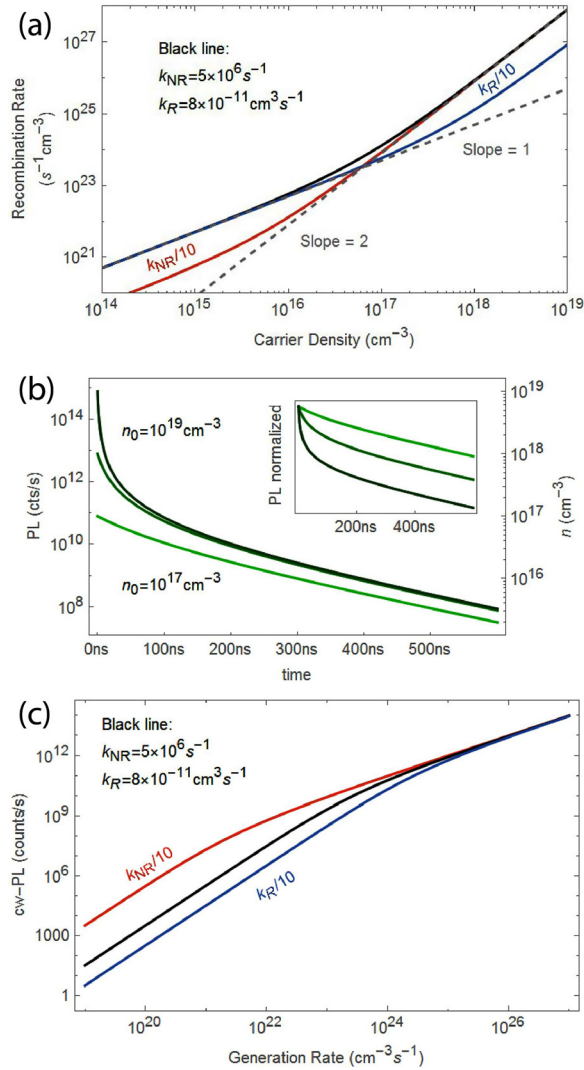


**FIG. 2.** Simulated photoluminescence following Eqs. (3) and (4). (a) Recombination rate ( $k_R n^2 + k_{NR} n$ ) for different carrier densities within the perovskite layer. The slope goes from 1 in the low-injection (non-radiative) regime to 2 in the high-injection (radiative) regime. Values for the black line are taken from Ref. 26. (b) tr-PL curves for different initial carrier densities. The quadratic regime is only visible at high density. (c) cw-PL as simulated by  $k_R n^2$  for different steady-state generation rates.

the excitation density ( $\Delta n$ ), as shown in Fig. 2(a), but the corresponding rate constants  $k_R$  and  $k_{NR}$  are not time- or excitation density-dependent. The rate constants can be determined by cw or tr-PL as described below.<sup>39,41,42</sup>

At excitation densities well above the trap density, the non-radiative losses in  $\Delta n$  are relatively small ( $R_R > R_{NR}$ ) so that  $\Delta n \approx \Delta p$ . Hence, if radiative recombination dominates (high carrier density), then  $d\Delta n(t)/dt \propto \Delta n^2$ , while in the non-radiative regime,  $d\Delta n(t)/dt \propto \Delta n$  (low carrier density), as shown in Fig. 2(a).

In a tr-PL measurement, the initial carrier density decays over time, and the measurement thus samples over a range of carrier densities, as visualized in Fig. 2(b). The rate constant can be obtained from

fitting the decays with Eq. (3). It should be noted that non-radiative recombination of charges reduces  $\Delta n(t)$  and consequently lowers the rate of radiative recombination ( $R_R$ ). Thus, a long PL lifetime does not necessarily indicate that all photo-generated charges are long-lived, as this may also be observed if the majority of charges is trapped.<sup>45,46</sup> Therefore, multiple excitation densities must be measured to get insights into the dominant recombination pathways.  $Q_e^{PL}$  gives additional insights into whether a long PL lifetime is associated with non-radiative losses. The main difference between cw-PL and tr-PL is that the carrier density in the steady-state measurement is fixed by the competition of generation and recombination rates. In quasi-equilibrium

$$\Delta n = \frac{k_{NR}}{2k_R} \left( -1 + \sqrt{1 + \frac{4Gk_R}{k_{NR}^2}} \right). \quad (4)$$

This means that in cw-PL, the intensity vs fluence (directly related to  $G$ ) is quadratic in the non-radiative regime and linear in the radiative regime, see Fig. 2(c). Thus, the fluence-dependence of cw-PL can in principle also be used to extract the values for  $k_R$  and  $k_{NR}$ . However, as visualized in Fig. 2(c), this often requires a very large range of excitation densities, at least 5–6 orders of magnitude for typical  $k_{NR}$  ( $5 \times 10^6 s^{-1}$ ) and  $k_R$  ( $8 \times 10^{11} cm^3 s^{-1}$ ) values in perovskites.<sup>26</sup> It is typically easier to obtain the rates from tr-PL as this requires only a few different initial excitation densities to extract the recombination rates [i.e., from the variation in lifetime, recall Fig. 2(b)]. We note that in mixed-halide perovskites, where phase segregation can lead to an inhomogeneous energy landscape, photodoping may possibly occur.<sup>47</sup> This additional doping can lead to (semi) first-order radiative recombination, if  $\Delta n \gg \Delta p$  (or  $\Delta p \gg \Delta n$ , recall Eq. (3)).

The rate constants  $k_R$  and  $k_{NR}$  obtained from fitting the tr-PL data can be used to determine  $\Delta n$  and  $\Delta p$  in steady-state (i.e.,  $V_{oc}$ ) conditions. Here,  $d\Delta n(t)/dt = 0$ , and the continuous illumination results in  $G$  being constant in time and thus constant in the values of  $\Delta n$  and  $\Delta p$  for a given illumination intensity. From here, the QFLS can be calculated, which gives an upper limit for  $V_{oc}$ . This approach therefore enables screening of various perovskite materials with transient excitation (and detection) techniques; this information can then be used to estimate the optimum  $V_{oc}$  in the corresponding devices.<sup>22,28</sup>

Insights into non-radiative pathways can also be obtained from other time-resolved spectroscopy techniques. To elucidate the nature of non-radiative recombination pathways at the perovskite-transport material interface, transient absorption spectroscopy (TAS)<sup>40</sup> or time-resolved conductivity (measured via microwave or THz absorption)<sup>48</sup> measurements are more suitable than tr-PL. While tr-PL offers insights into different radiative pathways and decreases in the PLQY due to non-radiative losses, it does not allow for distinguishing between different non-radiative pathways. Therefore, the combination of PL studies (both cw and tr) and other transient techniques is a powerful way to screen new materials for application as selective contacts in perovskite solar cells. However, we note that different transient techniques are typically performed at different excitation densities, which may make it difficult to extrapolate the results to the operational conditions of the solar cell.<sup>16</sup> For example, excitation densities in TAS or THz spectroscopy measurements on perovskites are typically  $>10^{17} cm^{-3}$ , which is several orders of magnitude larger than  $\sim 10^{15} cm^{-3}$  obtained by AM1.5 illumination. Hence, the recombination

processes often observed with TAS or THz spectroscopy, such as third-order Auger recombination [ $\sim \Delta n^3$ , ignored in Eq. (3)], are not necessarily relevant in the corresponding solar cell. Although it is difficult to probe charge recombination kinetics at PV-relevant conditions with THz spectroscopy, THz *emission* spectroscopy can be used to monitor charge separation dynamics (for instance at interfaces) and study surface defects.<sup>50,51</sup>

Time-resolved microwave conductivity (TRMC) and tr-PL, on the other hand, are useful techniques to access the relevant, lower excitation regimes of  $10^{14}$ – $10^{16}$  cm<sup>-3</sup>. TRMC measurements determine the charge carrier mobility and the lifetime of *mobile* charges and can thus be used to predict their diffusion in either the perovskite or the transport layer by measuring these layers individually.<sup>41,49</sup> The combination of TRMC and tr-PL is especially useful

since TRMC probes the recombination of all mobile charges, i.e., both radiative and non-radiative, while tr-PL selectively measures the radiative recombination lifetimes. Extensive analysis is however needed to differentiate the underlying physical processes corresponding to the observed kinetics. In a bilayer consisting of a perovskite and a transport layer for instance, a decreased PL lifetime could be due to charge transfer at the interface, but it can also be caused by fast trapping of charges by defects at the interface. The TRMC lifetimes distinguish between these processes since efficient charge separation results in infinitely long lifetimes of mobile charges, whereas interfacial recombination rapidly quenches mobile charges resulting in sub-ns lifetimes.<sup>48</sup>

With TAS measurements, the bleach of each layer that is populated with photo-generated charges can be probed as a function of

**TABLE I.** Summary of variables that can be studied with cw-Photoluminescence (cw-PL), time-resolved photoluminescence (TRPL), transient absorption spectroscopy (TAS), time-resolved microwave conductivity (TRMC), and THz spectroscopy and pros (+) and cons (–) of these techniques.

Technique	Reveals	Pros and Cons
cw-PL	<ul style="list-style-type: none"> <li>• Emission energy</li> <li>• PLQY</li> <li>• Photoluminescence quenching</li> <li>• <math>k_R</math> and <math>k_{NR}</math> for a wide range of illumination conditions</li> </ul>	<ul style="list-style-type: none"> <li>+ Simple</li> <li>+ Spectral information</li> <li>+ No full device needed</li> <li>- Wide range of intensities needed to get rate constants/not easy to access quantitative information</li> <li>- Loss channels not defined</li> <li>- Limited information</li> </ul>
TRPL	<ul style="list-style-type: none"> <li>• Lifetime quenching</li> <li>• Sensitive measurement of <math>k_R</math> and <math>k_{NR}</math> for layers without contacts</li> <li>• Information about surface recombination velocities for layers with contacts</li> <li>• Need to make sure that density is suitable to measure both rates</li> </ul>	<ul style="list-style-type: none"> <li>+ Relatively simple</li> <li>+ No full device needed</li> <li>- Interpretation not trivial</li> <li>- May require complementary measurements (numerical); a model is needed, especially for layers with contacts</li> <li>+ Spectral information</li> </ul>
TAS	<ul style="list-style-type: none"> <li>• Timescale for all processes</li> <li>• Transfer across junctions</li> <li>• Emission energy</li> <li>• ps to microsecond timescales</li> </ul>	<ul style="list-style-type: none"> <li>+ Probes non-radiative decay</li> <li>+ No full device needed</li> <li>- Complex measurement</li> <li>- High excitation density (<math>&gt; 10^{16}</math> cm<sup>-3</sup>)</li> </ul>
TRMC	<ul style="list-style-type: none"> <li>• Mobility of free charges</li> <li>• Lifetime of photo-conductivity</li> <li>• ns to millisecond timescales</li> </ul>	<ul style="list-style-type: none"> <li>+ Distinguish between charge transfer and interfacial recombination</li> <li>+ Low excitation density (<math>10^{13}</math> – <math>10^{17}</math> cm<sup>-3</sup>)</li> <li>+ No full device needed</li> <li>- Limited availability</li> <li>- Can only extract the product of carrier density and mobility</li> </ul>
THz spectroscopy	<ul style="list-style-type: none"> <li>• Mobility of free charges</li> <li>• Lifetime of photo-conductivity</li> <li>• ps to ns timescales</li> <li>• Charge separation (THz emission)</li> </ul>	<ul style="list-style-type: none"> <li>+ Distinguish between charge transfer and interfacial recombination</li> <li>+ No full device needed</li> <li>- High excitation density (<math>&gt; 10^{16}</math> cm<sup>-3</sup>)</li> <li>- Limited availability</li> <li>- Can only extract the product of carrier density and mobility</li> </ul>

time after excitation. This spectral resolution allows us to differentiate between charge dynamics in the perovskite and the transport layer. Hence, TAS can be used to discriminate between charge transfer, interfacial recombination, and trapping either inside the perovskite layer or in the transport layer, provided that the excitation densities are low enough and the energetic landscape is known.<sup>40</sup> Including non-radiative loss processes in the charge-transport layers in  $R_{NR}$  [Eq. (3)] enables us to predict the  $V_{oc}$  losses occurring both in the perovskite layer itself and at different interfaces.

Finally, we discuss routes toward finding selective transport layers in perovskite solar cells. In Table I, we summarize our discussion of cw-PL and transient techniques that can be applied for screening perovskite-transport layer structures and discriminating between radiative and non-radiative processes. The combination of cw- and tr-PL is a powerful approach to study both the magnitude (i.e., intensity in cw-PL) and rate (i.e., lifetime in tr-PL) of radiative recombination and will yield quantitative insights into non-radiative processes induced by interfacing the perovskite with a specific transport layer. Setups for cw-PL measurements are available in most device fabrication laboratories and can be quickly applied to screen whether a transport layer material induces changes in the perovskite PL. Considering that any quenching of the cw-PL by a transport layer means a loss in  $V_{oc}$ , the intensity and energy of cw-PL emission already give a good indication whether a transport layer introduces losses in the charge-carrier density or energy, respectively. However, the reduction in PL gives very limited insights into the loss channels, and it is not always possible to measure enough excitation densities with cw-PL to obtain quantitative information. In principle, cw-PL measurements can also be performed in full devices, away from  $V_{oc}$  conditions in order to identify losses occurring during carrier extraction.<sup>35</sup> Still, complete devices contain multiple interfaces, and isolating the influence of a single transport layer on performance losses is non-trivial.

With tr-PL, each interface can be assessed individually, by comparing the transients of perovskite layers and perovskite/transport layer bilayers. In addition, it is much easier to get information about the charge-carrier dynamics with tr-PL measurements than with cw-PL. However, the interpretation of tr-PL is not trivial, and multiple excitation densities and kinetic models are needed to understand the underlying recombination processes. Fitting the transients yields the rate constants for radiative and non-radiative recombination, which can be used to predict the upper limit of  $V_{oc}$  for a certain perovskite/transport layer combination. Finally, more advanced (but less available) tr-spectroscopy techniques such as TAS, TRMC, and THz spectroscopy can yield further insights into non-radiative carrier dynamics. Care, however, must be taken due to the differences in the excitation densities used for each measurement.

Currently, most state-of-the-art transport layers introduce non-radiative losses, as evidenced by the frequently-observed PL quenching in bilayers of the perovskite/transport layer, which significantly reduces the QFLS and thus  $V_{oc}$ .<sup>22,28</sup> Another limitation of frequently used (organic) transport layers in perovskite solar cells is their low conductivity, which limits the charge transport to the electrodes, reducing the fill factor ( $FF$ ) of the device.<sup>14</sup> Ideally, one would use a semiconducting transport layer and tune its conductivity via controlled doping, or else a very thin buffer layer, to avoid electrical losses. However, this is complicated by the fact that halide perovskites tend to react with metals and metal oxides<sup>52,53</sup> without suitable

functionalization.<sup>54</sup> Therefore, to maximize both  $FF$  and  $V_{oc}$ , future work should focus on optimizing the conductivity of the transport layer, while minimizing chemical reactivity and interfacial recombination.

The work of E.M.H. and B.E. is part of the Dutch Research Council (NWO) and was performed at the research institute AMOLF. T.K. acknowledges the Helmholtz Association for funding via the PEROSEED project. D.C. acknowledges funding from the Yotam project and the CNRS-Weizmann collaboration.

## REFERENCES

- A. Kojima, K. Teshima, Y. Shirai, and T. Miyasaka, *J. Am. Chem. Soc.* **131**, 6050 (2009).
- See <https://www.nrel.gov/pv/cell-efficiency.html>, for NREL efficiency chart (2020).
- H. Jin, E. Debroye, M. Keshavarz, I. G. Scheblykin, M. B. J. Roeflaers, J. Hofkens, and J. A. Steele, *Mater. Horiz.* **7**, 397–410 (2020).
- D. Luy, R. Su, W. Zhang, Q. Gong, and R. Zhu, *Nat. Rev. Mater.* **5**, 44 (2020).
- C. M. Wolff, P. Caprioglio, M. Stollerfoht, and D. Neher, *Adv. Mater.* **31**, 1902762 (2019).
- P. Schulz, D. Cahen, and A. Kahn, *Chem. Rev.* **119**, 3349 (2019).
- X. Ren, Z. S. Wang, and W. C. H. Choy, *Adv. Opt. Mater.* **7**, 1900407 (2019).
- B. Roose, Q. Wang, and A. Abate, *Adv. Energy Mater.* **9**, 1803140 (2019).
- R. Brendel and R. Peibst, *IEEE J. Photovoltaics* **6**, 1413 (2016).
- E. T. Roe, K. E. Egelhofer, and M. C. Lonergan, *ACS Appl. Energy Mater.* **1**, 1037 (2018).
- C. W. Tang and S. A. Vanslyke, *Appl. Phys. Lett.* **51**, 913 (1987).
- T. G. Allen, J. Bullock, X. Yang, A. Javey, and S. D. Wolf, *Nat. Energy* **4**, 914 (2019).
- P. K. Nayak, S. Mahesh, H. J. Snaith, and D. Cahen, *Nat. Rev. Mater.* **4**, 269 (2019).
- V. M. Le Corre, M. Stollerfoht, L. Perdigón Toro, M. Feuerstein, C. Wolff, L. Gil-Escrig, H. J. Bolink, D. Neher, and L. J. A. Koster, *ACS Appl. Energy Mater.* **2**, 6280 (2019).
- U. Rau, U. W. Paetzold, and T. Kirchartz, *Phys. Rev. B* **90**, 035211 (2014).
- I. Levine, S. Gupta, A. Bera, D. Ceratti, G. Hodes, D. Cahen, D. Guo, T. J. Savenije, J. Ávila, H. J. Bolink, O. Millo, D. Azulay, and I. Balberg, *J. Appl. Phys.* **124**, 103103 (2018).
- W. Shockley and H. J. Queisser, *J. Appl. Phys.* **32**, 510 (1961).
- J. Guillemales, T. Kirchartz, D. Cahen, and U. Rau, *Nat. Photonics* **13**, 501 (2019).
- J. Nelson, *The Physics of Solar Cells* (Imperial College Press, 2007).
- P. Würfel, *Physics of Solar Cells: From Basic Principles to Advanced Concepts* (Wiley-VCH, 2005).
- D. A. Neamen, *Semiconductor Physics and Devices*, 4th ed. (McGraw Hill, 2012).
- D. Guo, V. M. Caselli, E. M. Hutter, and T. J. Savenije, *ACS Energy Lett.* **4**, 855 (2019).
- U. Rau, *Phys. Rev. B* **76**, 085303 (2007).
- A. W. Walker, O. Höhn, D. N. Micha, B. Bläsi, A. W. Bett, and F. Dimroth, *IEEE J. Photovoltaics* **5**, 1636 (2015).
- O. D. Miller, E. Yablonovitch, and S. R. Kurtz, *IEEE J. Photovoltaics* **2**, 303 (2012).
- J. M. Richter, M. Abdi-Jalebi, A. Sadhanala, M. Tabachnyk, J. P. H. Rivett, L. M. Pazos-Outón, K. C. Gödel, M. Price, F. Deschler, and R. H. Friend, *Nat. Commun.* **7**, 13941 (2016).
- I. L. Braly, D. W. Dequillettes, L. M. Pazos-Outón, S. Burke, M. E. Ziffer, D. S. Ginger, and H. W. Hillhouse, *Nat. Photonics* **12**, 355 (2018).
- M. Stollerfoht, P. Caprioglio, C. M. Wolff, J. A. Márquez, J. Nordmann, S. Zhang, D. Rothhardt, U. Hörmann, Y. Amir, A. Redinger, L. Kegelmann, F. Zu, S. Albrecht, N. Koch, T. Kirchartz, M. Saliba, T. Unold, and D. Neher, *Energy Environ. Sci.* **12**, 2778 (2019).
- Z. Liu, L. Krückemeier, B. Krogmeier, B. Klingebiel, J. A. Márquez, S. Levchenko, S. Öz, S. Mathur, U. Rau, T. Unold, and T. Kirchartz, *ACS Energy Lett.* **4**, 110 (2019).

- <sup>30</sup>S. S. Shin, S. J. Lee, and S. I. Seok, *APL Mater.* **7**, 022401 (2019).
- <sup>31</sup>A. Zohar, M. Kulbak, I. Levine, G. Hodes, A. Kahn, and D. Cahen, *ACS Energy Lett.* **4**(1), 1 (2019).
- <sup>32</sup>J. Liu, S. Chen, D. Qian, B. Gautam, G. Yang, J. Zhao, J. Bergqvist, F. Zhang, W. Ma, H. Ade, O. Inganäs, K. Gundogdu, F. Gao, and H. Yan, *Nat. Energy* **1**, 16089 (2016).
- <sup>33</sup>S. M. Menke, N. A. Ran, G. C. Bazan, and R. H. Friend, *Joule* **2**, 25 (2018).
- <sup>34</sup>F. D. Eisner, M. Azzouzi, Z. Fei, X. Hou, T. D. Anthopoulos, T. J. S. Dennis, M. Heeney, and J. Nelson, *J. Am. Chem. Soc.* **141**, 6362 (2019).
- <sup>35</sup>M. Stolterfoht, V. M. Le Corre, M. Feuerstein, P. Caprioglio, L. J. A. Koster, and D. Neher, *ACS Energy Lett.* **4**, 2887 (2019).
- <sup>36</sup>K. Tvingstedt, O. Malinkiewicz, A. Baumann, C. Deibel, H. J. Snaith, V. Dyakonov, and H. J. Bolink, *Sci. Rep.* **4**, 6071 (2015).
- <sup>37</sup>T. Du, W. Xu, M. Daboczi, J. Kim, S. Xu, C. T. Lin, H. Kang, K. Lee, M. J. Heeney, J. S. Kim, J. R. Durrant, and M. A. McLachlan, *J. Mater. Chem. A* **7**, 18971 (2019).
- <sup>38</sup>A. Al-Ashouri, A. Magomedov, M. Roß, M. Jošt, M. Talaikis, G. Chistiakova, T. Bertram, J. A. Márquez, E. Köhnen, E. Kasparavičius, S. Levenco, L. Gil-Escrig, C. J. Hages, R. Schlattmann, B. Rech, T. Malinauskas, T. Unold, C. A. Kaufmann, L. Korte, G. Niaura, V. Getautis, and S. Albrecht, *Energy Environ. Sci.* **12**, 3356 (2019).
- <sup>39</sup>S. D. Stranks, V. M. Burlakov, T. Leijtens, J. M. Ball, A. Goriely, and H. J. Snaith, *Phys. Rev. Appl.* **2**, 034007 (2014).
- <sup>40</sup>K. Pydzińska, J. Karolczak, I. Kosta, R. Tena-Zaera, A. Todinova, J. Idígoras, J. A. Anta, and M. Ziólek, *ChemSusChem* **9**, 1647 (2016).
- <sup>41</sup>E. M. Hutter, G. E. Eperon, S. D. Stranks, and T. J. Savenije, *J. Phys. Chem. Lett.* **6**, 3082 (2015).
- <sup>42</sup>M. B. Johnston and L. M. Herz, *Acc. Chem. Res.* **49**, 146 (2016).
- <sup>43</sup>F. Staub, H. Hempel, J.-C. Hebig, J. Mock, U. W. Paetzold, U. Rau, T. Unold, and T. Kirchartz, *Phys. Rev. Appl.* **6**, 044017 (2016).
- <sup>44</sup>O. Gunawan, S. R. Pae, D. M. Bishop, Y. Virgus, J. H. Noh, N. J. Jeon, Y. S. Lee, X. Shao, T. Todorov, D. B. Mitzi, and B. Shin, *Nature* **575**, 151 (2019).
- <sup>45</sup>R. Brenes, D. Guo, A. Osherov, N. K. Noel, C. Eames, E. M. Hutter, S. K. Pathak, F. Niroui, R. H. Friend, M. S. Islam, H. J. Snaith, V. Bulović, T. J. Savenije, S. D. Stranks, V. Bulovic, and S. D. Stranks, *Joule* **1**, 155 (2017).
- <sup>46</sup>C. J. Hages, A. Redinger, S. Levchenko, H. Hempel, M. J. Koeper, R. Agrawal, D. Greiner, C. A. Kaufmann, and T. Unold, *Adv. Energy Mater.* **7**, 1700167 (2017).
- <sup>47</sup>S. Feldmann, S. Macpherson, S. P. Senanayak, M. Abdi-jalebi, J. P. H. Rivett, G. Nan, G. D. Tainter, T. A. S. Doherty, K. Frohna, E. Ringe, R. H. Friend, H. Sirringhaus, M. Saliba, D. Beljonne, S. D. Stranks, and F. Deschler, *Nat. Photonics* **14**, 123 (2020).
- <sup>48</sup>E. M. Hutter, J.-J. Hofman, M. L. Petrus, M. Moes, R. D. Abellón, P. Docampo, and T. J. Savenije, *Adv. Energy Mater.* **7**, 1602349 (2017).
- <sup>49</sup>J. E. Kroeze, T. J. Savenije, M. J. W. Vermeulen, and J. M. Warman, *J. Phys. Chem. B* **107**, 7696 (2003).
- <sup>50</sup>B. Guzelturk, R. A. Belisle, M. D. Smith, K. Bruening, R. Prasanna, Y. Yuan, V. Gopalan, C. J. Tassone, H. I. Karunadasa, M. D. McGehee, and A. M. Lindenberg, *Adv. Mater.* **30**, 1704737 (2018).
- <sup>51</sup>C. S. Ponseca, A. Arlauskas, H. Yu, F. Wang, I. Nevinskas, E. Du Da, V. Vaičaitis, J. Eriksson, J. Bergqvist, X. K. Liu, M. Kemerink, A. N. Krotkus, O. Inganas, and F. Gao, *ACS Photonics* **6**, 1175 (2019).
- <sup>52</sup>R. A. Kerner and B. P. Rand, *J. Phys. Chem. Lett.* **8**, 2298 (2017).
- <sup>53</sup>J. Yang, B. D. Siempelkamp, E. Mosconi, F. De Angelis, and T. L. Kelly, *Chem. Mater.* **27**, 4229 (2015).
- <sup>54</sup>Tulus, S. Olthof, M. Marszalek, A. Peukert, L. A. Muscarella, B. Ehrler, O. Vukovic, Y. Galagan, S. C. Boehme, and E. Von Hauff, *ACS Appl. Energy Mater.* **2**, 3736 (2019).